Study of momentum-transfer distributions in rotationally inelastic collisions of CO_2 with foreign gas perturbers*

William K. Bischel†
Department of Applied Science, University of California, Davis–Livermore, California 94550

Charles K. Rhodes†
Lawrence Livermore Laboratory, Livermore, California 94550

(Received 17 February 1976)

An experimental technique utilizing the methods of laser saturation spectroscopy that enables a direct observation of the momentum transfer distribution generated by rotationally inelastic molecular collisions is presented. This method has been applied to CO_2 in collision with a wide variety of partners including CO_2, H_2, Ne, NH_3, and CH_3F. The observations indicate that in a large number of cases the rotational transition results primarily from peripheral collisions which are effective in transferring angular momentum, but which communicate a relatively small linear momentum transfer.

I. INTRODUCTION

Fundamental knowledge concerning the detailed aspects of atomic and molecular collisions is of considerable scientific and practical importance. Although studies involving molecular beams[1] provide us with the most refined data, many other methods, including coherent spectroscopy[2] and the consideration of collisional effects on spectral line profiles[3,4] have been used. These latter techniques, although relatively simple to implement experimentally, are not sufficiently precise in the state selection of the colliding particles, and therefore are often insensitive to many details of the interaction potential. For example, total cross-section data do not exhibit interferences between partial waves, an aspect which is both an informative and striking characteristic of the angular distributions available from molecular-beam experiments.

Molecular interactions are complicated phenomena. One of the essential complexities arises from their normally noncentral nature, a fact which significantly multiplies both experimental and theoretical considerations.[5] The central and noncentral components of the potential differ, however, in an important way. Central forces are incapable of developing a torque and are, consequently, ineffective in producing transitions involving a change in the angular momentum of the colliding systems. Such transitions are generated entirely by the anisotropic component of the force field. A common example of this phenomenon is rotational relaxation of molecules in the gas phase. An understanding of these processes is important for a broad range of problems ranging from astrophysical[6] questions to coherent pulse propagation.[7]

We report below the characteristics of an experimental approach[8–10] which isolates some of the properties of the noncentral interaction of molecular systems. In this work we observe the linear momentum distribution generated by rotationally *inelastic* encounters of CO_2 with a variety of collision partners. From the previous discussion, the rotational inelasticity signifies the participation of the noncentral forces. We note that the extension of this experimental technique, which is one dimensional in nature, to three spatial dimensions will enable studies equivalent to molecular-beam investigations in the examination of differential scattering cross sections.

The general process under examination is

$$CO_2(j,\vec{v})+M \rightleftarrows CO_2(j',\vec{v}')+M\ ,$$

where the pair $(j,\vec{v})$ labels, respectively, the rotational quantum number and velocity of the CO_2 molecule, and M represents the appropriate collision partner. In the experimental technique described below, the methods of saturation spectroscopy are utilized to detect the velocity distribution arising from rotationally inelastic collisional processes and therefore provide an evaluation of the mean change of one component (z component) of the molecular velocity, viz., $(\vec{v}-\vec{v}')_z|_{av}\equiv\Delta v_z$, in these collisions. These data provide direct information on the characteristics of the intermolecular forces[5] and supplement the findings of alternative methods, such as pressure broadening and kinetic studies.[11] Previous studies examining the velocity dependence of collisions of atomic and molecular systems include molecular-beam experiments,[12] coherent spectroscopy,[2] determinations of infrared pressure-broadening coefficients,[13] and the role of velocity cross relaxation on the Lamb dip.[14] In this experiment, the initial

and final states of a collision-induced transition in a radiating molecule are monitored using the techniques of double-resonance spectroscopy.[15] These double-resonance techniques have yielded a surprising amount of information about molecular collisional processes. A partial list includes (1) collision rates between rotational levels[16] or vibrational levels,[17] (2) selection rules for various state-changing collisional processes,[15,18] (3) reorientational collision rates,[19,20] and (4) molecular velocity changes associated with specific collisional processes.[8-10]

The paper is organized in the following manner: A simple theoretical model describing the collision-induced double-resonance signal will be derived in Sec. II. Section III describes the experiment and some of the results. These results are analyzed in Sec. IV, which concludes with a brief summary.

II. THEORY OF COLLISION-INDUCED RESONANCE

Theoretical models for collisionally induced double resonance problems can be found in the work of Shoemaker *et al.*[19] and Johns *et al.*[20] for the case of a Stark-tuned system. Meyer *et al.*[8,21] also outlines a method to calculate the fluorescence intensity for the specific system discussed here. All of these theories start with a variation of the Boltzmann equation and include the effect of the saturating laser field as a perturbation on the system. The theory presented by Shoemaker and co-workers[19] uses a density matrix formalism. We propose here an alternative to the density matrix formalism and present an approximate model based on rate equations similar to those used by Johns *et al.*[20] We feel that this simpler method offers some advantages in clarity and physical interpretation.

A. Basic theory

Figure 1, which parallels the description of Freund *et al.*,[22] illustrates the theoretical model which will be considered in this section. The problem will be formulated in terms of a strong saturating field (Ω_1) and a weak signal field (Ω_2), as depicted in this figure. The saturating field creates a perturbation in its population distribution which is then transferred by collisions to the levels probed by the signal laser. Generalizations to the case of two strong fields can easily follow.

As we describe in Sec. III, our experiment actually observes the 4.3-μm fluorescence intensity of the $|00^01\rangle$ state in CO_2. Our signal therefore is a probe of the population distribution in velocity space of this level. Since we are modulating the two lasers at different frequencies and looking for a signal at the sum frequency, we will observe perturbations due only to the effect of *both* lasers. The theory which follows will try to reflect these experimental conditions as closely as possible.

In discussing the four-level problem, we will denote the population in the ith level (n_i) as a sum of the equilibrium population n_i^0 and its deviation from it, δn_i (i.e., $n_i = \delta n_i + n_i^0$). We also consider the velocity dependence of the population distribution by denoting $n_i(\beta)$, where $\beta = v/c$, such that $n_i(\beta)\, d\beta$ is the number of molecules in the ith level with velocity between β and $\beta + d\beta$. We then can calculate the change of molecular population, δn, brought about by the intense saturating field from the Karplus-Schwinger formula,[23]

$$\frac{\delta n_3(\beta)}{n_1^0(\beta)} = -\frac{\delta n_1(\beta)}{n_1^0(\beta)} = \frac{1}{2}\frac{(\mu_1 E_1/h)^2}{[\Omega_1(1-\beta)-\nu_{13}]^2 + (\frac{1}{2}\Delta\nu_1)^2 + (\mu_1 E_1/h)^2}\,, \tag{1}$$

where μ_1 is the transition dipole moment (~0.2 D for CO_2), ν_{13} is the transition frequency between levels 1 and 3, and $\Delta\nu_1$ is the full width at half-maximum (FWHM) collision-broadened width (~0.85 MHz for CO_2 at 100 mTorr). Here E_1 is the electric field amplitude of laser 1 and Ω_1 is defined as the laser frequency in hertz. Under our experimental conditions, $\mu_1 E_1/h \sim 0.7$ MHz, indicating that an appreciable number of molecules with ve-

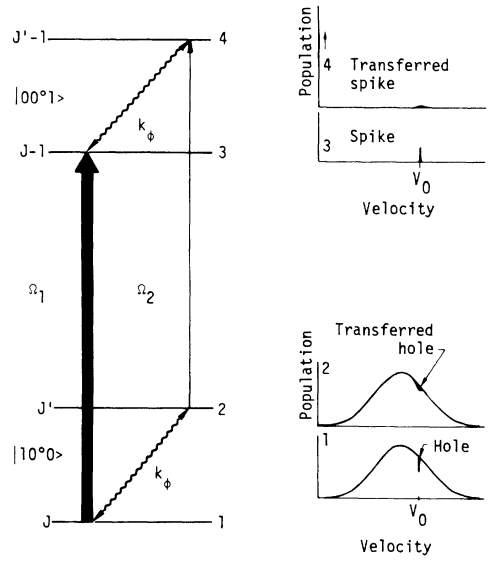

FIG. 1. Four-level collisional-induced double-resonance effect. A strong laser (labeled Ω_1) burns a "hole" in level 1 which is then transferred to level 2 by collisions at a rate k_ϕ. Level 2 is then probed by a weak laser (labeled Ω_2). Similar effects occur for levels 3 and 4.

locity such that $\Omega_1(1-\beta)=\nu_{13}$ are pumped from the ground level 1 to the excited level 3, leaving a "hole" in the velocity profile in the ground state and a "spike" in the upper state. This situation is illustrated in Fig. 1. This steady-state distribution is then communicated to other levels by collisions. We present here an extremely simple model for these collisional processes. The collision-induced transition rate from levels $1 \rightleftarrows 2$ and $3 \rightleftarrows 4$ is indicated by k_Φ and assumed to be equal. All other collision-induced transitions which connect levels 1, 2, 3, and 4 to the thermal bath are indicated by k_ℓ. In this model we will neglect elastic collisions, since they add nothing to the qualitative understanding of the solution. We also must consider the velocity changes accompanying collision-induced transitions. We describe the collision rate of transitions $1 \rightleftarrows 2$ and $3 \rightleftarrows 4$ with the molecules changing their velocity from β to β' by $k_\Phi \rho(\beta,\beta')$, where $\rho(\beta,\beta')$ is normalized such that

$$\int_{-\infty}^{\infty} \rho(\beta,\beta')\,d\beta' = 1 \ .$$

In this experiment we will assume that the radiating molecule can undergo collisions both with itself and with foreign gas perturbers. Therefore we generalize the rate equations presented by Johns *et al.*[20] to include these collisions leading to the equation for the steady-state population distribution of the ith state ($i=2$ or 4),

$$\frac{dn_i(\beta)}{dt} = \int_{-\infty}^{\infty} d\beta' \,[k_{\Phi x}(\beta')\rho_x(\beta',\beta) + k_{\Phi m}(\beta')\rho_m(\beta,\beta')]n_j(\beta') - (k_{\Phi x}+k_{\Phi m})n_i(\beta) + R_i(\beta) - (k_{\ell x}+k_{\ell m})n_i(\beta) = 0 \ , \tag{2}$$

where $R_i(\beta)$ is the term which describes the thermal pumping of the ith level and the subscripts $i,j=1,2$ or $3,4$. Here x refers to collisions between the radiating molecules and m refers to collisions between the radiating and the perturbing molecules. Note that the collision rates $k_{\Phi i}$ depend on the *partial* pressure of the ith gas and *not* on the total pressure.

In Eq. (2) we have left out the perturbation in the ith level (assuming $i=2$ or 4) generated by the Ω_2 radiation field, since its intensity is initially assumed to be weak. Using the principle of detailed balance and subtracting from Eq. (2) the thermal equilibrium contribution leads to the steady-state population difference (δn_i) transferred from level $1 \rightleftarrows 2$ or $3 \rightleftarrows 4$ as

$$\delta n_i(\beta) = \frac{1}{k_T}\int_{-\infty}^{\infty} d\beta' \,\delta n_j(\beta')[k_{\Phi x}\rho_x(\beta',\beta) + k_{\Phi m}\rho_m(\beta',\beta)] \ ,$$

where

$$k_T = (k_{\Phi x}+k_{\ell x}) + (k_{\Phi m}+k_{\ell m}) = k_x + k_m \ .$$

By conservation of energy, the intensity of the fluorescence signal is proportional to the amount of energy absorbed from the two laser fields. Assuming that the absorption coefficient α can be written

$$\Delta I_2/I_2 \cong \alpha_2 L \ ,$$

we see that the total energy absorbed per unit volume from the signal beam is

$$\Delta W = I_1 \alpha_2 L/c \ . \tag{4}$$

Our signal, however, stems only from the change in the absorption coefficient (α_2) owing to the collisionally transferred populations δn_2 and δn_4. Therefore using Eq. (4) and the usual equations for the absorption coefficient we obtain the contribution to the *change* in the total energy absorbed,

$$\Delta W(\beta) = \frac{-8\pi^2 \nu_{24}\mu_{24}^2(\frac{1}{2}\Delta\nu_2)[\delta n_2(\beta) - \delta n_4(\beta)]I_2 L/c}{3ch\{[\Omega_2(1-\beta)-\nu_{24}]^2 + [\frac{1}{2}\Delta\nu_2]^2 + [\mu_{24}E_2/h]^2\}} \ . \tag{5}$$

Equation (5) should be interpreted as the *variation* in the energy absorbed from the probe beam (E_2) owing to the perturbation caused by the pump beam (E_1) and *not* as the total energy absorbed. Remember that this expression was derived for a weak probe beam (i.e., $E_2 \to 0$) such that it did not affect the populations of levels 2 and 4. Normally, $E_1 \sim E_2$, and this is included to first order by inserting a power-broadening term $[(\mu_{24}E_2/h)^2]$ in the linewidth function in Eq. (5). Also, since this effect can be observed for either beam, a term identical to Eq. (5) with all subscripts interchanged (i.e., $1 \rightleftarrows 2$ and $3 \rightleftarrows 4$) must be added to $\Delta W(\beta)$. We can now calculate the total signal (ΔW_T) by substituting Eqs. (1) and (3) for δn_2 and δn_4, using the Maxwellian velocity distribution

$$n_j^0(\beta) = n_j^0(mc^2/2\pi kT)^{1/2} e^{-mc^2\beta^2/2kT}$$

and integrating over β. To perform this integration we assume that $k(\beta)$ and $e^{-mc^2\beta^2/2kT}$ are slowly varying functions of β, compared to the Lorentzian expressions in Eq. (5). These functions can then be treated as constants with $\beta=\beta_0$, where β_0 is determined by the position of the pump laser [i.e., $\Omega_1(1-\beta_0)=\nu_{13}$] and removed from the integral. The total signal can then be written

$$\Delta W_T = A(\beta_0)\left(\frac{k_{\Phi x}}{k_T}\int_{-\infty}^{\infty}\int_{-\infty}^{\infty} \rho_x(\beta,\beta')D_1(\beta')D_2(\beta)\,d\beta\,d\beta' + \frac{k_{\Phi m}}{k_T}\int_{-\infty}^{\infty}\int_{-\infty}^{\infty} \rho_m(\beta,\beta')D_1(\beta')D_2(\beta)\,d\beta\,d\beta'\right) \ , \tag{6}$$

where

$$A(\beta_0) = -(\pi hL/6c)(\nu_{24}\Delta\nu_2 n_1^0 + \nu_{13}\Delta\nu_1 n_2^0)e^{-mc^2\beta_0/2kT} \times (\mu_{13}E_1/h)^2(\mu_{24}E_2/h)^2(mc^2/2\pi kT)^{1/2}$$

and

$$D_j(\beta) = \{[\Omega_j(1-\beta)-\nu_j]^2 + (\tfrac{1}{2}\Delta\nu)^2 + (\mu E_j/h)^2\}^{-1} ,$$

where j denotes either transition 1 or 2. Here $\frac{1}{2}\Delta\nu$ is the total homogeneous pressure-broadened line width, and we have defined

$$I_2 = cE_2^2/8\pi .$$

Note that Eq. (6) assumes that both the probe and pump lasers are traveling in the same direction (indicated by the $1-\beta$ term). There are several interesting points to be made about Eq. (6). First, the signal goes as the product of the two laser intensities I_1 and I_2. This has been verified in Ref. 16 and in our experiment. Second, the intensity of this collision-induced resonance is governed by the factor k_Φ/k_T, which is the ratio of the rate of dip-transferring collisions Φ to the total inelastic collision rate. Hence one can obtain information about specific rate coefficients by monitoring relative intensities. This has been done in Ref. 20 for NH_3, H_2CO, and CH_3F.

The integration in Eq. (6) cannot be done analytically without assuming a general form for the velocity part of the collision kernel $\rho_i(\beta,\beta')$. Two limiting cases for $\rho_i(\beta',\beta)$ have been considered in the literature.[19,20]

Case 1. If the molecules change their rotational state withcut changing their velocity, we can approximate $\rho_i(\beta',\beta) = \delta(\beta',\beta)$, and the integrals in Eq. (6) reduce to

$$J = \int_{-\infty}^{\infty} \{[\Omega_2(1-\beta)-\nu_{24}]^2 + \Gamma_2^2\}^{-1} \times \{[\Omega_1(1-\beta)-\nu_{13}]^2 + \Gamma_1^2\}^{-1} d\beta , \quad (7)$$

where Γ_j is defined as $\Gamma_j^2 = (\frac{1}{2}\Delta\nu)^2 + (\mu E_j/h)^2$. Defining $\Delta_1 = \Omega_1 - \nu_{13}$, $\Delta_2 = \Omega_2 - \nu_{24}$, and assuming that $\Omega_1 \simeq \Omega_2 = \Omega$ (an approximation good to about 1 part in 300 for our case), we can evaluate the integral in Eq. (7), using contour methods, as[19,20]

$$J = (1/\Omega)(\pi^2/\Gamma_1\Gamma_2)G(\Delta_1,\Delta_2) , \quad (8)$$

where the normalized line-shape function $G(\Delta_1,\Delta_2)$ is a Lorentzian and is written

$$G(\Delta_1,\Delta_2) = (1/\pi)(\Gamma_1+\Gamma_2)/[(\Delta_1-\Delta_2)^2 + (\Gamma_1+\Gamma_2)^2] . \quad (9)$$

Case 2. If the velocities of the molecules change very much during a collision which results in changes of rotational state [i.e., the change in $\rho(\beta,\beta')$ is much slower than in the Lorentzian function in Eq. (6)], we can approximate $\rho(\beta,\beta) = \rho(\beta_{01},\beta_{02})$ and remove it from the integral. The integrals in Eq. (6) now lead to

$$J = \int_{-\infty}^{\infty}\int_{-\infty}^{\infty} \rho_i(\beta',\beta)D_1(\beta')D_2(\beta)\,d\beta'\,d\beta = \rho_i(\beta_{01},\beta_{02})\,\pi^2/\Omega_1\Omega_2\Gamma_1\Gamma_2 \quad (10)$$

where i denotes the appropriate collision partner x or m. Now the shape of the line is contained in $\rho(\beta_{01},\beta_{02})$ and the sharp Lorentzian feature of Eq. (7) is lost.

Intermediate case. For most cases of interest, there is some velocity change associated with a molecular collision. Hence we cannot approximate the collision kernel $\rho(\beta,\beta')$ by a δ function. This problem can be handled in several different ways, but here we will follow the treatment outlined in Ref. 19. To begin, one must assume some form of $\rho(\beta,\beta')$. Keilson and Storer[24] first addressed this problem when solving the Boltzmann equation for Brownian motion. Following their treatment, we choose the kernel $\rho(\beta,\beta')$ to be a symmetric function of an arbitrary linear combination of velocities,

$$\rho_i(\beta,\beta') = [1/(2\pi)^{1/2}\Delta\beta_i]\exp[-(\beta-\alpha_i\beta')^2/2\Delta\beta_i^2] \quad (11)$$

where $\Delta\beta_i$, with $i = x, m$, is the rms velocity change (z direction) associated with $x-x$ or $x-m$ collisions and is related to the rms thermal velocity in the z direction,

$$\beta_{\text{rms}} = (1/c)(kT/m)^{1/2} ,$$

by

$$(\Delta\beta_i)^2 = (1-\alpha_i^2)\beta_{\text{rms}}^2 .$$

It has been shown[24] that this value for $(\Delta\beta)^2$ leads to the proper thermal equilibrium conditions. Taking the limit as $\alpha \to 1$ $(\Delta\beta \to 0)$, we obtain a very narrow velocity distribution for the collision kernel which becomes the δ function $\delta(\beta,\beta')$ used in case 1.

Substituting Eq. (11) into Eq. (6) leads to integrals of the form

$$J_i = \int_{-\infty}^{\infty} d\beta\,\frac{D_2(\beta)}{(2\pi)^{1/2}\Delta\beta_i} \times \int_{-\infty}^{\infty} d\beta'\,D_1(\beta')\exp[-(\beta-\alpha_i\beta')^2/2\Delta\beta_i^2] . \quad (12)$$

Unfortunately, there is no closed-form solution for this integral, and it must be evaluated numerically. Our data are not sufficiently accurate to warrant such measures. However, we can arrive at an approximate solution which is accurate enough to analyze the qualitative features of our

data. For this we note that the form of the β' integral in Eq. (12) is strongly reminiscent of the Voigt profile,[25] suggesting that for $\Gamma_1 > \Omega\Delta\beta_i$ the β' integral can be approximated by a Lorentzian of the form

$$[(\Delta_1 - \Omega_1\beta)^2 + \Gamma_{1i}^2]^{-1} ,$$

where the β' velocity dependence of Eq. (12) has been included in Γ_{1i} such that

$$\Gamma_{1i}^2 = \Gamma_1^2 + (\Omega\Delta\beta_i)^2 ,$$

for which we have assumed $\alpha \simeq 1$. Γ_{1i} can be interpreted as the width of the transferred population perturbation stemming from the Ω_1 laser for the ith type of collision ($i = x, m$). This is then convoluted with another Lorentzian to determine the line shape. This leads to an integral similar to that discussed in case 1, except that now Γ_1 is replaced by Γ_{1i}. The integrals in Eq. (12) can now be evaluated, using Eq. (8), as

$$J_i = \frac{1}{\Omega}\frac{\pi^2}{\Gamma_{1i}\Gamma_2} G_i(\Delta_1, \Delta_2)$$

$$= \frac{1}{\Omega}\frac{\pi}{\Gamma_2\Gamma_{1i}}\frac{\Gamma_{Ti}}{(\Delta_1 - \Delta_2)^2 + \Gamma_{Ti}^2}, \tag{13}$$

where we have defined

$$\Gamma_{Ti} = \Gamma_2 + \Gamma_{1i} = \Gamma_2 + [\Gamma_1^2 + (\Omega\Delta\beta_i)^2]^{1/2} . \tag{14}$$

For the case where $\Gamma_1 > \Omega\Delta\beta$ (i.e., small velocity jumps), Eq. (14) can be rewritten

$$\Gamma_{Ti}^2 \simeq \Gamma_2^2 + 2\Gamma_2\Gamma_1 + \Gamma_1^2 + (\Omega\Delta\beta_i)^2$$
$$\simeq (\Gamma_1 + \Gamma_2)^2 + (\Omega\Delta\beta_i)^2 . \tag{15}$$

This is the "addition" formula suggested in Ref. 16 and will be used in the subsequent analysis to evaluate the velocity changes that occur during a rotationally inelastic molecular collision. Contrary to the assumptions used in deriving Eq. (15), our experimental velocity jumps are of the order of or larger than Γ. Nevertheless, we will use Eq. (15) in our analysis since it is a generous simplification of the theory (see the Appendix) and provides us with a useful method for determining estimates of the collisionally induced velocity changes.

The total signal from Eq. (6) can now be written

$$\Delta W_T = \frac{A\pi^2}{\Omega\Gamma_2}\left(\frac{k'_{\Phi x}}{k'_x + k'_m R}\frac{G_x(\Delta_1\Delta_2)}{\Gamma_{1x}} + \frac{k'_{\Phi m} R}{k'_x + k'_m R}\frac{G_m(\Delta_1, \Delta_2)}{\Gamma_{1m}}\right), \tag{16}$$

where $G_i(\Delta_1, \Delta_2)$ is defined by Eq. (13) and where we have defined a pressure-independent collision rate $k_i = P_i k'_i$ by defining the ratio of the partial pressures P_i of the radiating molecules to the perturbing molecules as

$$R = P_m/P_x .$$

Note that the line-shape function of Eq. (16) is the sum of two Lorentzians with different heights and different widths. Since our experiments measure the height and width of the *total* distribution, it is necessary that we obtain an expression for this width in terms of meaningful parameters. This is done in the Appendix, and only the result will be quoted here. From Eq. (A12), the linewidth of our collisionally induced double-resonance signal is

$$\Delta\nu_{\mathrm{FWHM}} = 2\{(\Gamma_1 + \Gamma_2)^2 + \tfrac{1}{2}\Omega^2[\Delta\beta_x^2(1 + C) + \Delta\beta_m^2(1 - C)]\}^{1/2}, \tag{17}$$

where C is a function of the ratio of the partial pressures defined by Eq. (A7) as

$$C = (1 - R')/(1 + R'), \tag{18}$$

where

$$R' = Rk'_{\Phi m}\Gamma_{Tx}\Gamma_{1x}/k'_{\Phi x}\Gamma_{Tm}\Gamma_{1m}$$

and has a value which ranges over $-1 \leq C \leq 1$. Note that Eq. (17) has the correct limiting values for $C = \pm 1$.

The case where the velocity jump is larger than the homogeneous width (i.e., $\Omega\Delta\beta > \Gamma$) can also be handled in an approximate form using the integral detailed in Eq. (10). For this limiting case we write the total signal from Eq. (6) as

$$\Delta W_T = \frac{A\pi^2}{\Omega^2\Gamma_1\Gamma_2}\left(\frac{k'_{\Phi x}}{k'_x + k'_m R}\rho_x(\beta_{01}, \beta_{02}) + \frac{k'_{\Phi m} R}{k'_x + k'_m R}\rho_m(\beta_{01}, \beta_{02})\right),$$

where $\rho_i(\beta, \beta)$ is defined by Eq. (11). Since the velocity changes in this experiment are typically of the order of $\frac{1}{10}$ of the thermal velocity or less, we can safely approximate $\alpha = 1$ in Eq. (11), leading to

$$\Delta W_T = \frac{A\pi^2}{\Omega\Gamma_1\Gamma_2}\frac{1}{(2\pi)^{1/2}} \times \left(\frac{k'_{\Phi x}}{k'_x + Rk'_m}\frac{\exp[-(\Delta_1 - \Delta_2)^2/2(\Omega\Delta\beta_x)^2]}{\Omega\Delta\beta_x} + \frac{Rk'_{\Phi m}}{k'_x + Rk'_m}\frac{\exp[-(\Delta_1 - \Delta_2)^2/2(\Omega\Delta\beta_m)^2]}{\Omega\Delta\beta_m}\right). \tag{19}$$

To find the experimental half-width of this line shape, we must again solve the equation

$$\tfrac{1}{2}G(0) = G(\Delta_{1/2})$$

for $\Delta_{1/2}$, where

$$G(\Delta) = Ae^{-(\Delta/\delta_x)^2} + Be^{-(\Delta/\delta_m)^2},$$

and where A, B, δ_i, and Δ are defined by Eq. (19). Unfortunately, this leads to a transcendental equation which must be solved numerically. It should be noted that most of the experimental velocity jumps reported here should be evaluated from Eq. (19). However, we have analyzed our data using Eq. (17), since it was felt that the error in $\Delta\beta_i$ will be small if C is considered as an adjustable parameter with limited physical significance.

B. Relative intensities

To obtain an order-of-magnitude estimate of the collision-induced transition rate k_Φ, we must first estimate the signal intensity for the case of both the pump and probe lasers on the same line. This also gives a measure of the power-broadened linewidth $(\Gamma_1 + \Gamma_2)$, which is necessary in the determination of the velocity jump per collision. Using an analysis similar to that presented in Ref. 20 we calculate the normal Lamb-dip signal[26] to be

$$\Delta W_{TL} = (A\pi^2/\Omega\Gamma_1\Gamma_2)G(\Delta_1, \Delta_2),$$

where

$$G(\Delta_1, \Delta_2) = (1/\pi)(\Gamma_1 + \Gamma_2)/[(\Delta_1 - \Delta_2)^2 + (\Gamma_1 + \Gamma_2)^2]. \tag{20}$$

All quantities in Eq. (20) are assumed to be evaluated for the same line. This expression is also valid for the case of foreign gas broadening if the $\frac{1}{2}\Delta\nu$ term in Γ_1 and Γ_2 is interpreted to be proportional to the total collision rate. We will now compare this intensity to the intensities of the collisionally induced double-resonance signals for the two limiting cases previously considered.

Case 1 ($\Omega\Delta\beta < \Gamma$). Taking the ratio of Eq. (16) to Eq. (20) at line center (i.e., $\Delta_1 = \Delta_2$), we have

$$\frac{\Delta W_T}{\Delta W_{TL}} = \frac{\Gamma_1(\Gamma_1 + \Gamma_2)}{k'_x + k'_m R}\left(\frac{k'_{\Phi x}}{\Gamma_{Tx}\Gamma_{1x}} + R\frac{k'_{\Phi m}}{\Gamma_{Tm}\Gamma_{1m}}\right). \tag{21}$$

For the case of $R \to \infty$, this easily leads to the evaluation of the ratio of the collisionally induced rotational transition rate $(k_{\Phi m})$ to the total rate (k_m) as

$$\frac{\Delta W_T}{\Delta W_{TL}} = \frac{\Gamma_1(\Gamma_1 + \Gamma_2)}{\Gamma_{Tm}\Gamma_{Tm}}\frac{k'_{\Phi m}}{k'_m}. \tag{22}$$

Case 2 ($\Delta\nu_D > \Omega\Delta\beta > \Gamma$). For this case, we take the ratio of Eq. (19) to Eq. (20) at line center, resulting in

$$\frac{\Delta W_T}{\Delta W_{TL}} = \frac{\pi}{(2\pi)^{1/2}}\frac{\Gamma_1 + \Gamma_2}{k'_x + Rk'_m}\left(\frac{k'_{\Phi x}}{\Omega\Delta\beta_x} + \frac{Rk'_{\Phi m}}{\Omega\Delta\beta_m}\right). \tag{23}$$

Taking the limit as $R \to \infty$, we again have for the relative intensities

$$\frac{\Delta W_T}{\Delta W_{TL}} = \left(\frac{\pi}{2}\right)^{1/2}\frac{\Gamma_1 + \Gamma_2}{\Omega\Delta\beta}\frac{k'_{\Phi m}}{k'_m}. \tag{24}$$

This is the formula used in Sec. III to estimate the $\Delta J = 2$ collision-induced transition rate for CO_2-H_2 collisions.

III. FOUR-LEVEL EXPERIMENT

A. Apparatus

The experimental technique involved in the generation of a perturbed velocity distribution of a particular rotational level and the detection of the collisional transfer of this perturbation to a nearby rotational state is illustrated in Fig. 1. A saturating electric field from a CO_2 source, operating at a fixed frequency on a given 10.6-μm $P(J)$ transition (in our case $P20$ at + 12 MHz) is used to generate a nonequilibrium distribution in the $|10^00, J\rangle$ level of the CO_2 absorber gas. Inelastic rotational collisions transfer this perturbed distribution to other rotational states in this manifold. Similiar processes occur in the upper 00^01 level. If one now uses another CO_2 source to frequency scan the Doppler profile of one of these nearby rotational states, the perturbed velocity distribution of this level can be detected.

A diagram of the experimental apparatus necessary to perform these double-resonance experiments is given in Fig. 2. Four stable CO_2 sources are necessary and are operated in two probe/local-oscillator pairs (1,2) and (3,4). The two labeled 1 and 4 serve as local oscillators: by heterodyning them with their respective probes in helium-

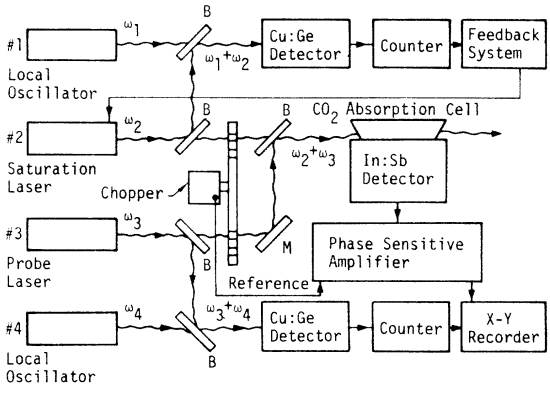

FIG. 2. Schematic diagram of the experimental apparatus, illustrating the two pairs 1, 2 and 3, 4 of stable probes and local CO_2 oscillators operating on $P(j)$ and $P(j')$ transitions, respectively. The probe beams ω_2 and ω_3 are combined by a beam splitter (B) and pass in spatial coincidence through the absorption cell. Modulation of the two probe beams is provided by the chopper. The oscillator frequencies are established by heterodyne techniques.

cooled Cu:Ge detectors, the frequency measurements $|\omega_1 - \omega_2|$ and $|\omega_3 - \omega_4|$ are established. The two beams originating from oscillators 2 and 3 are collinearly combined with a beam splitter and passed through an absorption cell which contains a gaseous mixture of CO_2 and the collision partner M. The pressures of the gases in the absorption cell are accurately measured with a capacitive manometer. Under typical experimental conditions, oscillator 2 is locked to a specified frequency within its gain profile by a frequency-counter feedback system. The intensity of both beams ω_2 and ω_3 entering the cell is approximately 20 W/cm^2. A large mirror at the bottom of the absorption cell collects the 4.3-μm fluorescence arising from the $CO_2(00^01 \rightarrow 00^00)$ transition and focuses it through a sapphire window at the top of the cell into a liquid-nitrogen-cooled In:Sb detector. The 4.3-μm fluorescence is observed by mechanically chopping the ω_2 beam at 780 Hz, the ω_3 beam at 540 Hz, and detecting synchronously at the sum frequency of 1320 Hz. At the same time oscillator 3 is scanned in frequency by applying a dc ramp voltage to the piezoelectric translator locating its output mirror. This technique ensures that only the component of the fluorescence due to the combined interaction of both radiation fields is detected. Both the fluorescent intensity and the frequency of oscillator 3 are simultaneously recorded on magnetic tape for subsequent numerical data reduction.

B. Experimental results

This experimental arrangement was used to examine the velocity changes in collisions of CO_2 with itself and the foreign gas perturbers of H_2, Ne, NH_3, and CH_3F. An analysis of the dominant term in the intermolecular potential indicates that these collision partners will provide a wide range of interactions from which some general conclusions can be drawn as to the effectiveness of cer-

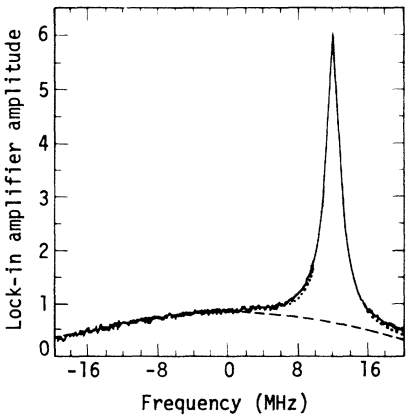

FIG. 3. Saturated resonance observed in 4.3-μm CO_2 fluorescence (40 mTorr of CO_2) using the apparatus of Fig. 2. Both oscillators were set on the 10.6-μm $P(20)$ transition. Oscillator 1 is swept through the resonance. The fitted width (indicated by the dotted line) is approximately 2 MHz.

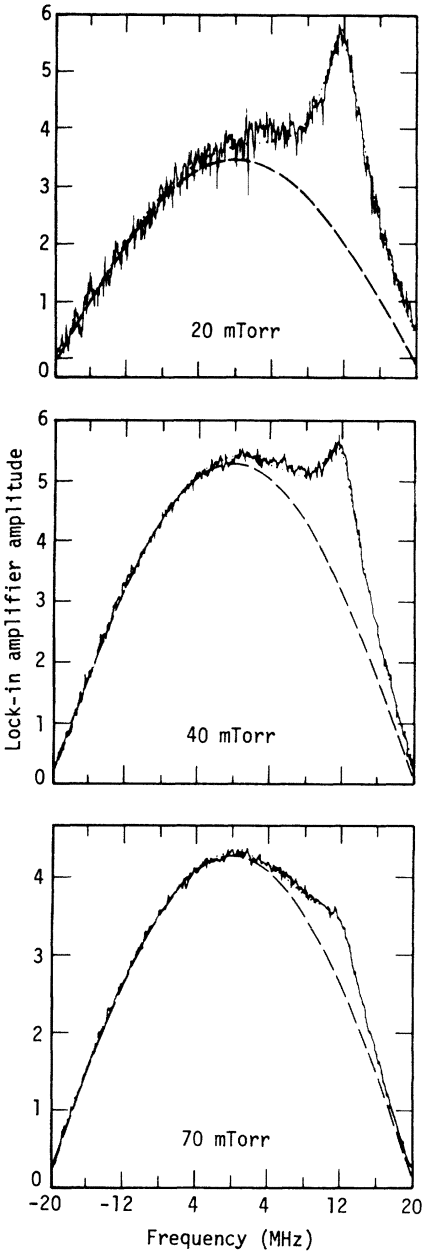

FIG. 4. Comparison of data taken for the four-level double-resonance experiment in pure CO_2 at three different pressures. Here the dotted line is a Gaussian plus Lorentzian (centered at +12 MHz) fitted to the total signal. The dashed line is the computer-determined Gaussian background contribution to the total signal. All fitted widths are ~6 MHz.

tain types of intermolecular forces in causing velocity changing collisions.

Figures 3 and 4 illustrate typical data obtained with this experimental method for pure CO_2 at a pressure of 40 mTorr. In Fig. 3, a narrow two-level resonance is exhibited when both lasers 2 and 3 are operated on the 10.6-μm $P(20)$ transition. Laser 2 is locked 12 MHz above the $P20$ line center for this data. The FWHM of this resonance is 2.1 ± 0.1 MHz and is primarily determined by power broadening. This width corresponds to $\Gamma_1 + \Gamma_2$ in Eq. (20).

Figure 4 exhibits the nature of the four-level signal when source 2 is set to a specified frequency on the 10.6-μm $P(20)$ transition while source 3 is scanned across the 10.6-μm $P(18)$ transition. Included in this figure are data taken at three different pressures, illustrating the effect of pressure on the four-level resonance signal. Note that the fitted widths for these resonances are approximately three times as broad as the width of the resonance in Fig. 3, indicating that the molecular velocity has changed appreciably during the rotationally inelastic collision. Both of these resonances were fitted using a numerical computer fitting routine. Here the dotted line is the best fit to a Gaussian centered at line center (determining the background contribution to the total signal) plus a Lorentzian centered at + 12 MHz (determining the collision-induced contribution to the total signal). The height and width of this Lorentzian are then recorded for subsequent data analysis. Note that the problem of the background signal which limited the accuracy of the results in Ref. 8 has been solved by taking the data at a laser frequency which does not correspond to line center, thus creating an asymmetric total signal. All of the fitted widths for the self-broadening case were approximately 6 MHz. Using Eq. (17) with $R = 0$ and determining $\Gamma_1 + \Gamma_2$ from data similar to Fig. 4 gives a value for the rms velocity change per collision in CO_2 of 2.8 cm/sec. This value will subsequently be used to determine the velocity jumps due to the foreign gas perturbers.

The signal in Figs. 4 and 5 was determined by contributions from both the upper and lower states. We report additional measurements isolating the contribution of the rotational levels in the upper (00^01) state, an effect which was below the detectable limit in the earlier studies of Ref. 8. This refinement was obtained through improvements in the experimental conditions which resulted in a substantially increased signal-to-noise ratio.

For the experimental configuration illustrated in Fig. 2, the influence of the 00^01 level is isolated when oscillator 2 is operated on the 10.6-μm $P(20)$ transition and oscillator 3 is operated on

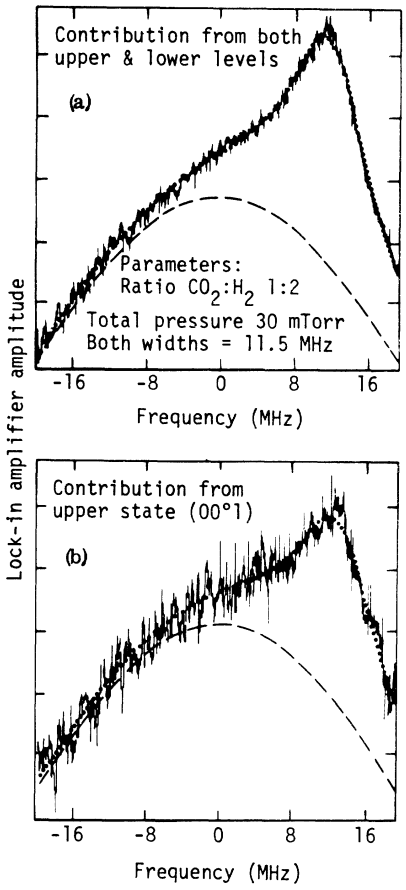

FIG. 5. Comparison of four-level resonance in CO_2-H_2 mixtures with partial-pressure ratios of $P_{H_2}/P_{CO_2} = 2$ for (a) oscillator 2 on the 10.6-μm $P(20)$ line and oscillator 3 on the 10.6-μm $P(18)$ line and (b) isolating the contribution to the collision-induced signal from the upper state. Note that in this case both widths are the same, indicating that the velocity changes are not sensitive to the particular CO_2 excited state.

the 9.6-μm $P(18)$ transition. No contribution from the lower 10^00 and 02^00, levels is expected under these conditions, since the $10^00 \rightleftharpoons 02^00$ collisional rate is much less than that associated with rotational transfer, and essentially complete velocity redistribution will be generated in collisionally induced transitions between these two states.[27] Data demonstrating this effect are shown in Fig. 5, which corresponds to a gas mixture composed of a 2:1 ratio of H_2 to CO_2 at a total pressure of 30 mTorr. Figure 5(a) is the contribution from both upper and lower levels, while Fig. 5(b) isolates the contribution from just the upper $|00^01\rangle$ state. The resonant feature centered at 12 MHz is clearly visible and has a measured width of ~11.5 MHz. This result is attributed entirely to rotationally inelastic processes occurring in the 00^01 manifold. Note that the widths of Figs. 5(a)

TABLE I. CO_2-H_2 data dependence on the ratio of the partial pressures.

Ratio P_{H_2}/P_{CO_2}	$\frac{C}{1-Rk}{1+Rk}$	Theory $\Delta\nu_{FWHM}$	Expt. $\Delta\nu_{FWHM}$	Parameters used for theory
0	1.0	6.0	6.0 ± 1	
0.5	+0.43	8.9	9.3 ± 1	Refer to Eq. (17)
1	+0.16	10.0	10.3 ± 1	$\Gamma_1 + \Gamma_2 = 1.4$ MHz
2	−0.23	11.5	11.3 ± 1	$\Omega\Delta\beta_x = 2.6$ MHz
4	−0.52	12.5	12.4 ± 1	$\Omega\Delta\beta_m = 6.8$ MHz
6	−0.66	12.9	12.7 ± 1	$k = 0.80$
7	−0.70	13.0	13.4 ± 1	
11	−0.80	13.3	13.2 ± 1	
∞	−1.0	13.9	...	

and 5(b) are the same, indicating that the z component of the velocity change does not depend to first order on the vibrational state of the radiating molecule.

Since the CO_2-H_2 collisional system was extensively studied using these experimental techniques, we will use these data to compare to the theoretical model developed in Sec. II. We begin by comparing the ratio dependence of the partial pressures predicted by Eq. (17) to our experimental results. This is done in Table I and the results are plotted in Fig. 6. Here the circles are the experimental points and the solid line is the theoretical prediction of Eq. (17) using the parameters listed in Table I. Note that the data are fitted extremely well by a very sensitive function of the ratio of the partial pressures of two gases. Here

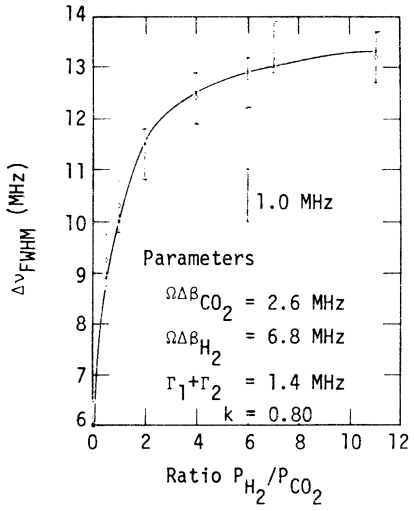

FIG. 6. Ratio dependence of CO_2-H_2 data for the four-level resonance. The solid line is the theoretical prediction of Eq. (17), using the listed parameters. The experimental points indicated by the circles are taken from Table I.

the pressure dependence is neglected since this comprises a very small portion of the total linewidth. If, on the other hand, we keep the ratio of the partial pressures constant and vary the pressure, Eq. (17) predicts that the linewidth will remain approximately constant, varying only slightly because of the pressure-broadening contribution to Γ. These data are shown in Fig. 7 for the two different ratios (P_{H_2}/P_{CO_2}) of 7 and 1. Here the slope of the line agrees with the slope measured from the power-broadening measurements (both lasers on the same line) and is approximately 10–12 MHz/Torr. Care must be taken not to interpret this slope as the CO_2-H_2 pressure-broadening coefficient, since our simple model indicates [see Eq. (1)] that the broadened width ($\Delta\nu$) and the power-broadened width ($\mu E/h$) add as the sum of the squares. The interested reader is referred to the work of Meyer *et al.*[21] for detailed methods of deconvolving the pressure-broadened slope from power-broadened linewidths.

We have also taken data for the foreign gas perturbers of Ne, NH_3, and CH_3F. Figure 8 compares the signals obtained using these three collision partners at roughly the same CO_2-M collision frequency. A comparison of the signal heights and widths indicated in Fig. 8 affords a particularly graphic demonstration of the fact that longer-range intermolecular force fields can be extremely efficient in transferring angular momentum (i.e., causing a rotational state change) and yet transfer very little linear momentum in the process. The fact that long-range forces easily transfer angular momentum can be understood using a classical model similar to one proposed in Ref. 7. Since the change in the angular momentum is equal to the torque applied during a collision, we see that for a given force field, the longer the lever arm (effective interaction radius), the larger the torque. This leads to the anticipated result that long-range intermolecular forces are the most effective in

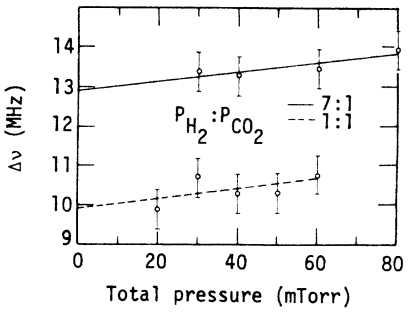

FIG. 7. Comparison of the pressure dependence of CO_2-H_2 collision-induced linewidths for two different ratios of the partial pressures. The fitted slope for the two cases is roughly 10–12 MHz/Torr.

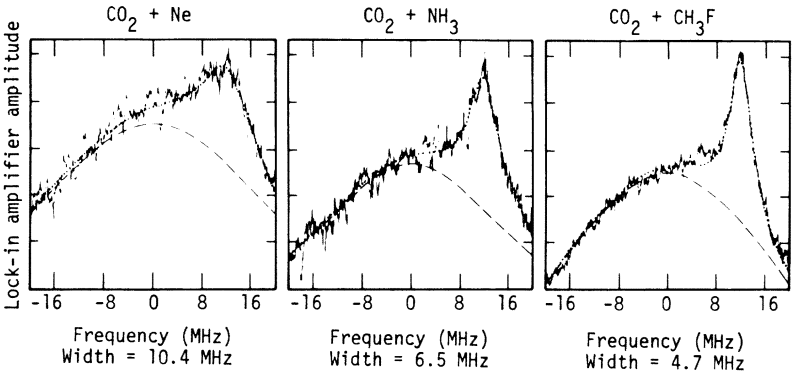

FIG. 8. Comparison of signals obtained for the three collision partners Ne, NH_3, and CH_3F. Note that the velocity change associated with the short-range forces of CO_2-Ne collisions give appreciably larger velocity changes that the longer-range dipole-quadrupole forces of CO_2-NH_3 and CO_2-CH_3F collisions.

transferring angular momentum. An analogous argument indicates that the longer-range forces are less effective in transferring linear momentum. In fact, velocity changes as small as 85 cm/sec (~0.1% of the thermal velocity) have been reported[2] for the long-range dipole-dipole collisions in CH_3F. These results explain the qualitative features of Fig. 8, since the dispersion forces for CO_2-Ne collision are of much shorter range than the dipole-quadrupole forces of CO_2-NH_3 and CO_2-CH_3F collisions.

CO_2 velocity changes for these collision partners were obtained by taking data at two different partial-pressure ratios and solving Eq. (17) for the values of $\Omega\Delta\beta_m$ and k. These values are listed in Table II. Unfortunately, the data were taken at only one ratio for CO_2-Ne collisions and hence a value of k had to be assumed in Eq. (17). Since the value of k seems to lie between 0.8 and 0.9 (See Table II), we arbitrarily choose the value of $k = 0.85$ to determine the order-of-magnitude value for this velocity change. We recall, however, that the adjustable parameter k does not possess a rigorous physical significance in this region, since we are in the region where the velocity jumps are larger than the power-broadened linewidth.

A brief investigation has also been made of the dependence of the four-level collision-induced resonance on the value of $|J - J'|$. For the case of CO_2 in collision with H_2, the velocity-selective resonance has been observed for $|J - J'| = 2$, 4, and 6, but was not detected for $|J - J'| > 6$. The signal intensities, however, are extremely small for $\Delta J > 2$. This observation is related to data obtained from the line-broadening studies, which can be used to estimate the maximum orbital angular momentum l_{max} operative in the collision. This is accomplished by relating the change in angular momentum to the product of the reduced mass of the collision partners, their relative velocities, and their interaction cross section determined line-broadening studies. For the CO_2-H_2 cross section of 7.4×10^{-15} cm^2 we find that $l_{max} \cong 14$. Thus for CO_2-H_2 collisions at 300 °K, $l_{max} = 6$ is a value which is consistant with our observations. In all other cases investigated, the resonance was observed only for $|J - J'| = 2$.

TABLE II. rms Δv_z velocity changes for CO_2-M collisions.

Collision Partner (M)	Velocity jump per collision ($\times 10^3$ cm/sec)	$k = R'/R$
CO_2	2.8 ± 0.6	...
H_2	7.2 ± 1.0	0.80
Ne	5.8 ± 2.0	0.85 [a]
NH_3	4.0 ± 0.8	0.85
CH_3F	1.6 ± 0.4	0.94

[a] Assumed value.

IV. DISCUSSION AND CONCLUSIONS

A. Transition rates and selection rules

Calculations of collision-induced transition rates are very similar to calculations involved in the determination of pressure-broadened linewidths. Anderson's theory[28] has had the most impact in this area. However, Oka[29] attempted theoretical calculations using Anderson's theory for modeling collision-induced transitions for his microwave double-resonance experiments. The results of these calculations were in marked disagreement with his measurements. Clearly new theoretical advances had to be made. Rabitz and Gordon,[30] using an approach similar to Anderson's but using the transition probabilities as calculated by a semiclassical perturbation theory carried to second order, calculated the transition rates for l-type doublets in HCN with good agreement with his measurements. Other attempts include one by Prakash and Boggs,[31] who tried modeling the experiments of Oka using an approach based on a recent theory for pressure broadening proposed by Murphy and Boggs.[11] They obtained reasonable

agreement with Oka's measurements, considering the experimental error in his results. All of these theoretical approaches expand the intermolecular potential in a multipole expansion, keeping at most only the first few terms. These theories obtain the best agreement with experiment when considering the long-range forces.

Although the experiments described here could provide new information on ratios of these collision-induced transition rates [see Eq. (24)], the relative intensities of the data reported here are not of sufficient accuracy to allow a determination of these ratios. Only the CO_2-H_2 system has enough data to estimate the ratio of the $\Delta J = \pm 2$ collision rate to the total inelastic collision rate by using Eq. (24). These estimates indicate that the majority (approaching 90%) of all CO_2-H_2 inelastic collisions change the CO_2 angular momentum by ±2 units. This fact is also supported by the observations reported in Sec. III of extremely weak signal intensity for $\Delta J > 2$ and no signal for $\Delta J > 6$.

These results tend to confirm the proposal that $\Delta J = 2$ is the preferred selection rule for these collisions. This quadrupole selection rule is the one which would be derived if it was assumed that the first term in the multipole expansion for the CO_2-H_2 collision system dominates the series. A general discussion of the selection rules for these collision-induced rotational transitions can be found in the review article by Oka.[15]

B. Velocity changes

As can be seen from Table II, the velocity changes seem to follow the general and expected rule that the shorter range the intermolecular force, the larger the velocity change. One notable counterexample is the case of CO_2-CO_2 collisions. Note from Table II that these velocity changes are smaller than every case investigated other than CO_2-CH_3F. This anomalous behavior exhibited by CO_2 indicates that a simple multipole expansion cannot adequately explain the velocity changes, and one must now allow for exchange processes not present for foreign gas perturbers. Very little theoretical work has been done in this area, because the collision process is extremely complex.

C. Evaluation of theoretical model

The simple theory presented in Sec. II appears to predict the qualitative features extremely well. It has also been very useful in providing a method by which the velocity change per collision can be deduced from the linewidth of the double-resonance signal. There are, however, several improvements that should be made if more accurate data warranted the additional effort. First, the theory should be reformulated so that differences in relaxation rates of the participating levels are taken properly into account. This can be done either with rate-equation or density matrix formalisms. Second, the radiation field should not be considered as a perturbation on the equilibrium population distribution, since a saturating laser field can change the populations of these levels by a factor of 2. Third, integrals such as Eq. (12) should be evaluated numerically in order to obtain the correct velocity changes to the intermolecular forces through the use of *ab initio* calculations, such as those which have been attempted for pressure-broadening coefficients.

D. Summary

In summary, a new experimental technique has been developed enabling a direct observation of the momentum transfer distribution in rotationally inelastic molecular collisions. With this method, velocity-selective rotational transfer has been detected for CO_2 in collision with CO_2, H_2, Ne, NH_3, and CH_3F. Specifically, for H_2 and CO_2 the data indicate values of $(\Delta v_z)_{av}$ for $J = 20 \rightleftarrows J' = 18$ transitions at 300 °K which are far less than the mean thermal speed. These data provide direct information on the anisotropic component of the intermolecular interaction and also demonstrate that collision-induced transitions between closely spaced levels can occur with a small effect on the molecular velocity for states that have no transition dipole moment. This is an extension of the conclusion reached by Anderson[28] for cases involving a transition dipole moment.

ACKNOWLEDGMENT

The authors would like to acknowledge the expert technical assistance of B. Schleicher.

APPENDIX: WIDTH FOR THE SUMMATION OF TWO LORENTZIAN LINES

Starting from Eq. (16), we have the collisionally induced double-resonance line-shape function

$$G(\Delta) = A/(\Delta + W_x) + B/(\Delta + W_m), \tag{A1}$$

where we have defined

$$\Delta = (\Delta_1 - \Delta_2)^2,$$

$$W_i = \Gamma_{Ti}^2 = (\Gamma_1 + \Gamma_2)^2 + (\Omega \Delta\beta_i)^2,$$

$$A = k'_{\Phi x} W_x / \Gamma_{Tx} \Gamma'_{1x} (k'_x + k'_m R),$$

$$B = R k'_{\Phi m} W_m / \Gamma_{Tm} \Gamma'_{1m} (k'_x + k'_m R).$$

Here R is defined as the ratio of the partial pressures, $R = P_m/P_x$. The other constants have been

defined in Sec. II.

The half width at half-maximum of any distribution function is defined by

$$G(\Delta_{1/2}) = \tfrac{1}{2}G(0). \tag{A2}$$

Solving this equation for $G(\Delta_{1/2})$, defined in Eq. (A1), we have

$$\frac{(\Delta_{1/2}+W_m)A + (\Delta_{1/2}+W_x)B}{(\Delta_{1/2}+W_x)(\Delta_{1/2}+W_m)} = \frac{1}{2}\frac{AW_m + BW_x}{W_m W_x}. \tag{A3}$$

This equation can be put into normal quadratic form, leading to

$$\Delta_{1/2}^2 + D\Delta_{1/2} + E = 0, \tag{A4}$$

where

$$D = W_x + W_m - 2W_x W_m(A+B)/(AW_m + BW_x),$$

$$E = -W_x W_m.$$

Substituting for A and B, D can be rewritten

$$D = W_x + W_m - [2/(1+R)](W_x + R'W_m), \tag{A5}$$

where R' is a function of the ratio of partial pressures, defined as

$$R' = R(k'_{\Phi m}/k'_{\Phi x})\Gamma_{Tx}\Gamma'_{1x}/\Gamma_{Tm}\Gamma'_{1m}. \tag{A6}$$

Now breaking W_i up into its components by using Eq. (A1), we have $W_i = \Gamma + \delta_2$, where $\Gamma = (\Gamma_1 + \Gamma_2)^2$ and $\delta_i = (\Omega\Delta\beta_i)^2$. Substituting these into Eq. (A5), we have

$$D = 2\Gamma + \delta_x + \delta_m - [2/(1+R')](\Gamma + \delta_x + R\Gamma + R\delta_m),$$

leading to

$$D = [(1-R')/(1+R')](\delta_m - \delta_x) = C(\delta_m - \delta_x). \tag{A7}$$

Here C is a convenient constant whose values range over $-1 \le C \le 1$ and which contains the total ratio dependence of the linewidth. We now calculate $\Delta_{1/2}$ from Eq. (A4):

$$\Delta_{1/2} = \tfrac{1}{2}[-D \pm (D^2 + 4E^2)^{1/2}]$$

$$= \tfrac{1}{2}C(\delta_x - \delta_m) + \{[C^2(\delta_x - \delta_m)^2 + 4(\Gamma + \delta_x)(\Gamma + \delta_m)]^{1/2}\}, \tag{A8}$$

where we have chosen the + sign because the value of Eq. (A8) must always be positive to give a real linewidth. Equation (A8) can be rewritten

$$\Delta_{1/2} = \tfrac{1}{2}\{C(\delta_x - \delta_m) + [(2\Gamma + \delta_m)^2 + (1-C^2)(\delta_x - \delta_m)^2]^{1/2}\}. \tag{A9}$$

Note that this expression has the correct limiting values for $C = \pm 1$. If $C = 1$, there is no foreign gas perturber and the linewidth is $\Delta_{1/2} = \Gamma + \delta_x$. For $C = -1$, the system is very dilute with only $x - m$ collisions. Here Eq. (A9) predicts the linewidth to be $\Delta_{1/2} = \Gamma + \delta_m$. If we assume the last term in Eq. (A9) is small compared to $2\Gamma + \delta_x + \delta_m$, $\Delta_{1/2}$ can be written

$$\Delta_{1/2} \simeq \tfrac{1}{2}[C(\delta_x - \delta_m) + 2\Gamma + \delta_x + \delta_m + (1-C^2)(\delta_x - \delta_m)^2/2(2\Gamma + \delta_x + \delta_m)]. \tag{A10}$$

This is the correct expression for the linewidth to first order. Assuming that the last term in (A10) is negligible, the value for the linewidth reduces to

$$\Delta_{1/2} = \Gamma + \tfrac{1}{2}[\delta_x(1+C) + \delta_m(1-C)]. \tag{A11}$$

This gives value for the full width at half-maximum of the experimentally observed linewidth as

$$\Delta\nu_{\mathrm{FWHM}} = 2\{(\Gamma_1 + \Gamma_2)^2 + \tfrac{1}{2}\Omega^2[\Delta\beta_m(1+C) + \Delta\beta_m^2(1-C]\}^{1/2}. \tag{A12}$$

From this expression, one can deduce $\Delta\beta_m$ if $\Delta\beta_x$ and $\Gamma_1 + \Gamma_2$ are known. An alternate approach is to go to high ratios ($C \to -1$); then the linewidth will reflect $\Delta\beta_m$ directly.

---

*Work partially performed under the auspices of the U. S. Energy Research and Development Administration.

† Present address: Molecular Physics Center, Stanford Research Institute, Menlo Park, Calif. 94025.

[1] *Molecular Beam Scattering* (Faraday Division of the Chemical Society, London, 1973).

[2] J. Schmidt, P. R. Berman, and R. J. Brewer, Phys. Rev. Lett. 31, 1103 (1973); Paul R. Berman, J. M. Levy, and Richard G. Brewer, Phys. Rev. A 11, 1968 (1975).

[3] P. R. Berman, Phys. Rev. A 6, 2157 (1972).

[4] A. P. Kolchenko, A. A. Pukhov, S. G. Rautian, and A. M. Shalagin, Zh. Eksp. Teor. Fiz. 63, 1173 (1973) [Sov. Phys.-JETP 36, 619 (1973)].

[5] M. L. Goldberger and K. M. Watson, *Collision Theory* (Wiley, New York, 1964); M. A. D. Fluendy, I. H. Kerr, and K. P. Lawley, Mol. Phys. 28, 69 (1974).

[6] C. H. Townes, in *Fundamental and Applied Laser Physics*, edited by M. S. Feld, A. Javan, and N. A. Kurnit (Wiley, New York, 1973), p. 739.

[7] F. H. Hopf and C. K. Rhodes, Phys. Rev. A 8, 912 (1973).

[8] Thomas W. Meyer and Charles K. Rhodes, Phys. Rev. Lett. 32, 637 (1974).

[9] Thomas W. Meyer, William K. Bischel, and Charles K. Rhodes, Phys. Rev. A 10, 1433 (1974).

[10] William K. Bischel and Charles K. Rhodes, in *Proceedings of the Ninth International Conference on the Physics of Electronic and Atomic Collisions*, edited by J. S. Riley and R. Geballe (Univ. of Washington Press, Seattle, 1975).

[11] Joseph Murphy and James E. Boggs, J. Chem. Phys.

47, 691 (1967); R. G. Gordon, J. Chem. Phys. 44, 3083 (1966).
[12]R. B. Bernstein, and J. T. Muckerman, in *Advances in Chemical Physics*, edited by J. O. Hirschfelder (Interscience, New York, 1967), Vol. 12.
[13]A. T. Mattick, A. Sanchez, N. A. Kurnit and A. Javan, Appl. Phys. Lett. 23, 12 (1973).
[14]Charles Freed, and Herman A. Haus, IEEE J. Quantum Electron. QE-9, 219 (1973).
[15]T. Oka, in *Advances in Atomic and Molecular Physics*, edited by D. R. Bates and I. Estermann (Academic, New York, 1973), Vol. 9.
[16]Ralph R. Jacobs, Kenneth J. Pettipiece, and Scott J. Thomas, Appl. Phys. Lett. 24, 375 (1974).
[17]I. O. Hocker, M. A. Kovacs, C. K. Rhodes, G. W. Flynn, and A. Javan, Phys. Rev. Lett. 17, 223 (1966); Ralph R. Jacobs, Kenneth J. Pettipiece, and Scott J. Thomas, Phys. Rev. A 11, 54 (1975).
[18]Ralph R. Jacobs, Scott J. Thomas, and Kenneth J. Pettipiece, IEEE J. Quantum Electron. QE-10, 480 (1975).
[19]R. L. Shoemaker, S. Stenholm, and Richard G. Brewer, Phys. Rev. A 10, 2037 (1974).
[20]J. W. C. Johns, A. R. W. McKellar, T. Oka, and M. Romheld, J. Chem. Phys. 62, 1488 (1975).
[21]Thomas W. Meyer, Charles K. Rhodes, and Herman A. Haus, Phys. Rev. A 12, 1993 (1975).
[22]S. M. Freund, J. W. C. Johns, A. R. W. McKellar, and T. Oka, J. Chem. Phys. 59, 3445 (1973).
[23]Robert Karplus and Julian Schwinger, Phys. Rev. 73, 1020 (1948).
[24]J. Keilson and J. E. Storer, Q. Appl. Math. 10, 243 (1952).
[25]For a discussion of the Voigt profile, see S. S. Penner, *Quantitative Molecular Spectroscopy and Gas Emissivities* (Addison Wesley, London, 1959); Allan C. G. Mitchell and Mark W. Zemansky, *Resonance Radiation and Excited Atoms* (Cambridge U. P., Cambridge, 1934).
[26]For a discussion of the derivation of the Lamb dip, see W. E. Lamb, Phys. Rev. 134, A1429 (1964); J. L. Hall, *The Line Shape Problem in Laser Saturated Molecular Absorption* (Institute for Theoretical Physics, University of Colorado, 1969) (unpublished). Our expressions follow closely those derived in Ref. 17.
[27]For a discussion of the appropriate vibrational transfer rates, see P. K. Cheo, in *Lasers*, edited by A. K. Levine and A. J. DeMaria (Dekker, New York, 1971), Vol. 3, p. 111.
[28]P. W. Anderson, Phys. Rev. 76, 647 (1949).
[29]T. Oka, J. Chem. Phys. 47, 13 (1967); Takeshi Oka, J. Chem. Phys. 48, 4919 (1968).
[30]H. A. Rabitz and R. G. Gordon, J. Chem. Phys. 53, 1815 (1970).
[31]Vinod Prakash and James E. Boggs, J. Chem. Phys. 57, 2599 (1972).